JOURNAL OF SOLID STATE CHEMISTRY 135, 111–115 (1998)
ARTICLE NO. SC977606

Site Occupancy Wave and Unprecedented Infinite Zigzag $(Te_2^{2-})_n$ Chains in the Flat Te Nets of the New Ternary Rare Earth Telluride Family ALn_3Te_8

Rhonda Patschke,* Joy Heising,* Jon Schindler,† Carl R. Kannewurf,† and Mercouri Kanatzidis*,[1]

*Department of Chemistry, Michigan State University, East Lansing, Michigan 48824; and †Department of Electrical Engineering and Computer Science, Northwestern University, Evanston, Illinois 60208

Received June 25, 1997; accepted September 2, 1997

The three isostructural compounds $CsCe_3Te_8$, $RbCe_3Te_8$, and KNd_3Te_8 were synthesized from the reaction of elemental copper and lanthanides in a molten alkali metal/polytelluride flux. They crystallize in the monoclinic space group $P2_1/a$ (No. 14) with $a = 9.057(2)$ Å, $b = 12.996(3)$ Å, $c = 14.840(3)$ Å, $\beta = 98.74(2)^\circ$, $V = 1726.4(7)$ Å^3, and $Z = 4$ for $CsCe_3Te_8$; $a = 9.051(2)$ Å, $b = 12.996(3)$ Å, $c = 14.376(3)$ Å, $\beta = 98.87(2)^\circ$, $V = 1670.8(7)$ Å^3, and $Z = 4$ for $RbCe_3Te_8$; and $a = 8.956(1)$ Å, $b = 12.836(2)$ Å, $c = 13.856(3)$ Å, $\beta = 99.42(1)^\circ$, $V = 1571.3(3)$ Å^3, and $Z = 4$ for KNd_3Te_8. The structure of all three compounds can be described as a defect $NdTe_3$ type, consisting of an anionic $Ln_3Te_8^-$ layer that is charge balanced with A^+ cations. The anionic layer contains a square Te lattice net with an unprecedented ordered defect pattern site occupancy wave. Variable-temperature electrical conductivity and thermopower measurements are reported.
© 1998 Academic Press

Key Words: **rare earth; flux synthesis; polytelluride; conductivity; thermopower.**

Many high-symmetry, low-dimensional compounds contain stacking layers that can be described as square lattice networks composed of one element. Examples include compounds of the Cu_2Sb structure type (1), the related ZrSiSe structures (2), the PbO and anti-PbO structures (3), the $BaAl_4$ (4), $ThCr_2Si_2$ (5), and $CaBe_2Ge_2$ (6) structure types, the $SrZnSb_2$ structure (7), and other less popular structure types (8). The chemical, physical, and electronic properties of these compounds are largely decided by these square nets and by their interaction with the remaining part of the structure. However, only a few are known for tellurium, e.g., $LnTe_2$, Ln_2Te_5, and $LnTe_3$ (9), $CsTh_2Te_6$ (10), $K_{0.33}Ba_{0.67}AgTe_2$ (11), and Cs_3Te_{22} (12). These square nets can have different electronic structures, which can lead to instabilities and structural distortions within the nets (13). These distortions are associated with several interesting physical phenomena such as charge density waves and anomalies in the charge transport properties. When the formal oxidation state of all Te atoms in the net is -2, a stable square net is observed (e.g., NaCuTe) (14). However, when the formal oxidation state is less than -2 or when there are atomic vacancies in the square net, structural distortions are possible leading to Te···Te bonding interactions and the formation of Te_x^{n-} species. These distortions are manifested through the formation of a superstructure with respect to the ideal square net (11). Here, we describe the synthesis and electrical properties of the compounds ALn_3Te_8 (A = Cs and Rb, Ln = Ce; A = K, Ln = Nd), which display a defect square Te net and an unprecedented intense charge density wave that leads to infinite zigzag $(Te_2^{2-})_n$ chains and (Te_3^{2-}) anions. Interestingly, this charge density wave has recently been predicted on theoretical grounds (15, 16), and this report constitutes the first experimental confirmation.

The three isostructural compounds ALn_3Te_8 (A = Cs and Rb, Ln = Ce; A = K, Ln = Nd) resulted from investigations into the A/Cu/Ln/Te (Ln = Ce, Nd) systems. Their two-dimensional structure is shown in Fig. 1. The Ln and Te atoms make up the anionic layers and the alkali cations reside in the interlayer gallery. The Ln atoms possess three crystallographic positions with two distinct coordination environments, shown in Fig. 2. Two of the Ln atoms are eight-coordinate with a bicapped trigonal-prismatic environment of Te. The third Ln atom is nine-coordinate with a tricapped trigonal-prismatic environment of Te.

The anionic layer of these compounds is a derivative of the $NdTe_3$ structure type, differing only in the occupancy of the square Te net. From a fully occupied $NdTe_3$ lattice, one tellurium atom is removed, causing the remaining Te atoms to "condense" into Te_3^{2-} oligomers and zigzag $(Te_2^{2-})_n$ polymers arranged in an unusual pattern, shown in Fig. 3. The bonding in the zigzag chains consists of almost equal Te–Te distances of 2.989(3) and 3.010(3) Å for $CsCe_3Te_8$. The

[1]To whom correspondence should be addressed. E-mail: kanatzidis@cemvax.cem.msu.edu.

0022-4596/98 $25.00
Copyright © 1998 by Academic Press
All rights of reproduction in any form reserved.

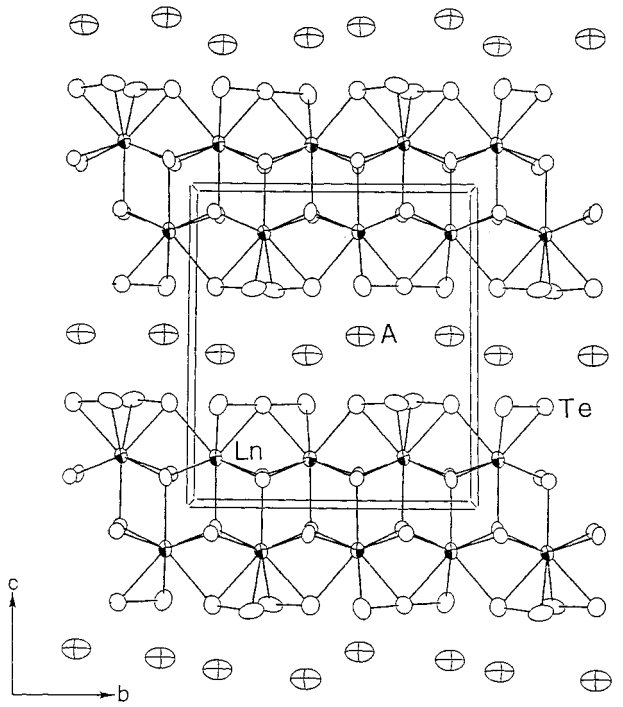

FIG. 1. Extended structure of ALn_3Te_8 as seen parallel to the anionic layer (circles with nonshaded octants: A = Cs, Rb, K; large open circles: Te; circles with shaded octants: Ln = Ce, Nd).

Te–Te distances in the trimerized Te_3^{2-} unit are 2.836(3) and 2.847(3) Å, longer than the normal Te–Te bond length of 2.76 Å found in $(Ph_4P)_2Te_4$ (17). The formal oxidation states are therefore $A^+(Ln_3Te_3)^{3+}(Te_3^{2-})(Te_2^{2-})_n$. The structure we observe for the defect square net in ALn_3Te_8 can be thought of as a 2×3 superstructure (in the a–b plane) of the $NdTe_3$ structure, which is thought to have an ideal square sublattice.

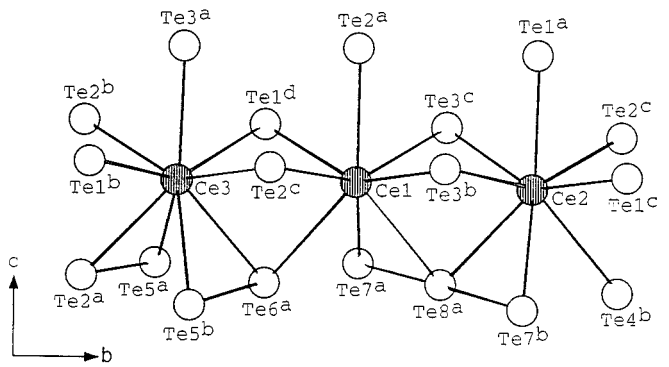

FIG. 2. A fragment of $CsCe_3Te_8$ showing the coordination environment of the Ln atoms. Selected distances (Å): Ce1–Te1^d = 3.244(3), Ce1–Te2^a = 3.296(3), Ce1–Te7^a = 3.356(3), Ce2–Te3^b = 3.249(3), Ce2–Te3^c = 3.251(3), Ce2–Te8^a = 3.278(3), Ce2–Te4^b = 3.337(3), Ce3–Te3^a = 3.298(3), Ce3–Te6^a = 3.317(3), Ce3–Te4^a = 3.323(3).

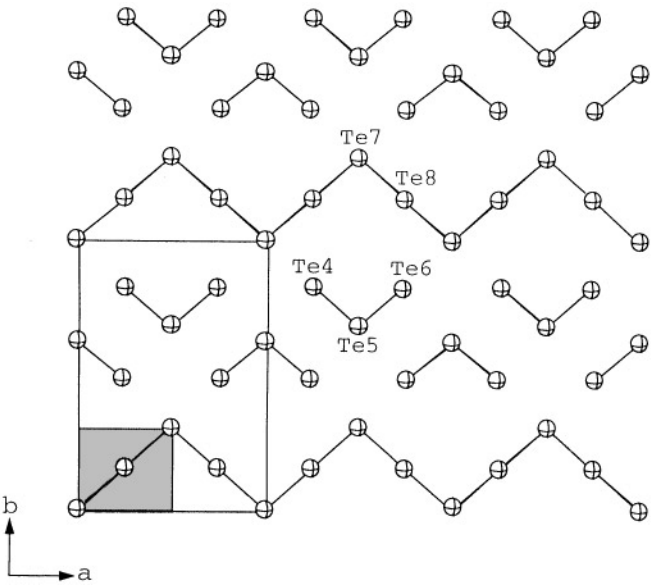

FIG. 3. View of the Te "net" of $CsCe_3Te_8$ showing the Te_3^{2-} units and the infinite zigzag $(Te_2^{2-})_n$ chains. The shaded area indicates the unit cell of the hypothetical parent structure of $NdTe_3$. The Te square net in the $NdTe_3$ structure is, of course, fully occupied. Selected distances (Å): Te4–Te5 = 2.837(3), Te6–Te5 = 2.847(3), Te7–Te8 = 2.989(3), Te6–Te8 = 4.284(2), Te6–Te7 = 3.297(3), Te4–Te7 = 3.317(3), Te4–Te8 = 4.277(2), Te5–Te6 = 3.510(3). Selected angles (deg): Te8–Te7–Te8 = 98.03(7), Te4–Te5–Te6 = 99.84(8), Te4–Te6–Te5 = 52.22(7), Te4–Te7–Te8 = 85.57(7), Te4–Te7–Te6 = 90.80(8).

The pattern of the Te net in ALn_3Te_8 was previously predicted on theoretical grounds by Lee and Foran (15) in reporting the structure of $RbDy_3Se_8$ (16). This compound was solved in a disordered model in the orthorhombic space group $Cmcm$ with $a = 4.0579(6)$ Å, $b = 26.47(1)$ Å, $c = 3.890(9)$ Å, but Weissenberg and precession photographs indicated a very weak superstructure with $a_{super} = 4a_{sub}$, $b_{super} = 3b_{sub}$, $c_{super} = c_{sub}$. This superstructure could not be resolved crystallographically. HOMO–LUMO energy calculations were made using Hückel theory to predict the superstructure pattern of $RbDy_3Se_8$. Although the 2×3 superstructure of ALn_3Te_8 is different from the 4×3 superstructure found in $RbDy_3Se_8$, one of the two lowest energy patterns predicted for the Se net in its superstructure is depicted in the Te net of ALn_3Te_8. Again the term "superstructure" here is used with respect to that of $NdTe_3$.

Electron diffraction studies on KNd_3Te_8 revealed an additional, possibly *incommensurate*, superstructure along the a axis. The reflections associated with this new superstructure are very weak and occur along the a^* direction with $a^*_{super} = 0.429a^*_{sub}$, where a_{sub} is the length of the KNd_3Te_8 cell (i.e., 8.956 Å). An optical densitometric scan obtained from electron diffraction photographs of the (hk0) reciprocal

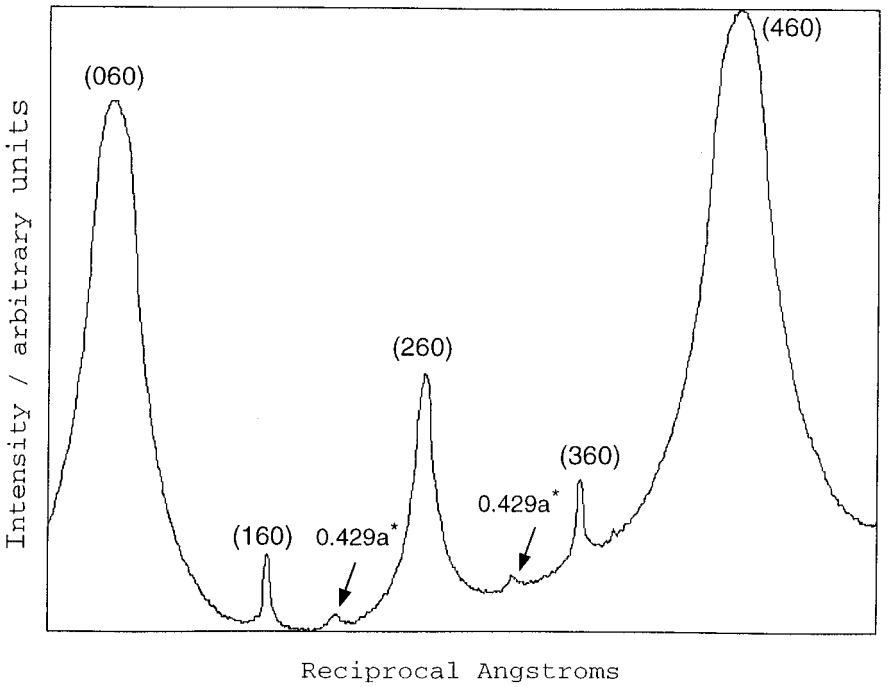

FIG. 4. An intensity scan obtained from an electron diffraction micrograph of KNd_3Te_8 along the (h60) row of reflections. The five reflections from the lattice of KNd_3Te_8 are indexed. The two weak peaks are from the superlattice with $a_{super} = 2.33a_{sub}$.

plane along the (h60) row of reflections is shown in Fig. 4. The weak reflections between the (160), (260), and (360) reflections are due to the additional $0.429a^*_{sub}$ superlattice, which corresponds to a $2.33 \times a_{sub}$ (i.e., $\sim$21 Å) lattice dimension. These results suggest an additional oligomerization and/or fragmentation along the chains of the Te trimers and/or the infinite zigzag chains, the origin of which is not currently understood.

Electrical conductivity data as a function of temperature for single crystals of KNd_3Te_8 show that the material is a semiconductor with a room temperature value of 0.1 S/cm; see Fig. 5A. The conductivity drops with falling temperature but, interestingly, the data do not follow the typical thermally activated behavior of semiconductors, suggesting a complicated electronic band structure at the Fermi level. The $CsCe_3Te_8$ could not be obtained in large enough single crystals to measure electrical conductivity. Hot-pressed pellets of this material, however, are only slightly less conductive than KNd_3Te_8. The faster decline of the conductivity at lower temperatures is due to grain boundaries in the pellet.

Thermoelectric power data obtained on KNd_3Te_8 and $CsCe_3Te_8$ show a very large Seebeck coefficient at room temperature of 500 and 400 μV/K, respectively. The decreasing Seebeck coefficient with decreasing temperature, its positive sign, and its large magnitude (see Fig. 5B) confirm that these compounds are p-type, narrow-gap semiconductors.

The magnetic susceptibilities of $RbCe_3Te_8$ and KNd_3Te_8 were measured over the range 5–300 K at 5000 and 6000 G, respectively. A plot of $1/\chi_M$ vs T for each shows that the material exhibits nearly Curie–Weiss behavior with only slight deviation from linearity beginning below 50 K. Such deviation has been reported for several Ln^{3+} compounds and has been attributed to crystal field splitting of the cation's $^2F_{5/2}$ (Ce^{3+}) and $^4I_{9/2}$ (Nd^{3+}) ground state. At temperatures above 150 K, a μ_{eff} of 2.76 μ_B for $RbCe_3Te_8$ and 3.33 μ_B for KNd_3Te_8 has been calculated. These values are in accordance with the usual range for Ce^{3+} (2.3–2.5 μ_B) and Nd^{3+} (3.5–3.62 μ_B) compounds.

EXPERIMENTAL PROCEDURE

1. **$CsCe_3Te_8$** was synthesized from a mixture of Cs_2Te (0.5 mmol), Cu (0.5 mmol), Ce (0.5 mmol), and Te (3.0 mmol) that was sealed under vacuum in a Pyrex tube and heated to 550°C for 4 days followed by cooling to 100°C at 4°C h^{-1}. The excess Cs_xTe_y flux was removed with DMF to reveal black hexagonal-shaped plate crystals. The crystals seem water stable but are air-sensitive when finely ground.

X-ray structural analysis of $CsCe_3Te_8$: crystal dimensions $0.178 \times 0.027 \times 0.089$ mm, monoclinic, $P2_1/a$ (No. 14), $Z = 4$, $a = 9.057(2)$ Å, $b = 12.996(3)$ Å, $c = 14.840(3)$ Å, $\beta = 98.74(2)°$, $V = 1726.4(7)$ Å^3, $\rho_{calc} = 6.056$ g cm^{-3}, $2\theta_{max} = 50°$, Mo$K\alpha$ radiation, $\lambda = 0.71069$ Å, ω–2θ scan mode,

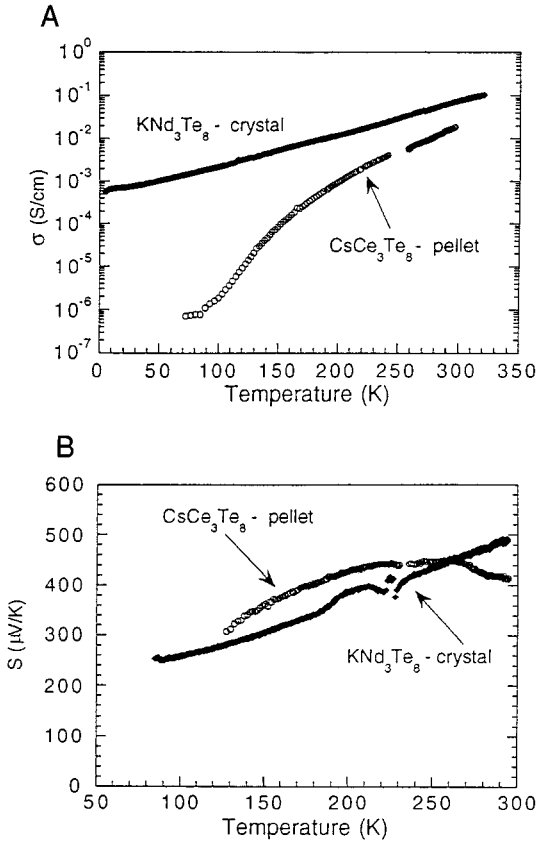

FIG. 5. (A) Single-crystal electrical conductivity [$\log\sigma$ (S/cm)] plotted against temperature (K) for KNd_3Te_8 and $CsCe_3Te_8$. (B) Thermopower (μV/K) plotted against temperature (K) for KNd_3Te_8 and $CsCe_3Te_8$.

$T = 23°C$, 3412 reflections measured, 3193 unique reflections, data corrected for Lorentz–polarization effects and for absorption (based on ψ scans), $\mu(MoK\alpha) = 232.41\,cm^{-1}$, solution by direct methods, anisotropic refinement on F by full-matrix least squares, 110 parameters, $R = 0.049$, $R_w = 0.063$ for 1591 reflections having $F_o^2 > 3\sigma(F_o^2)$, min/max residual electron density $= -3.8\,e\,Å^{-3}/4.5\,e\,Å^{-3}$.

2. **$RbCe_3Te_8$** was synthesized from a mixture of Rb_2Te (1.0 mmol), Cu (0.5 mmol), Ce (1.0 mmol), and Te (3.0 mmol) that was sealed under vacuum in a carbon-coated quartz tube and heated to 600°C for 3 days and then 850°C for 5 days, followed by cooling to 100°C at $4°C\,h^{-1}$. The excess Rb_xTe_y flux was removed with DMF to reveal black hexagonal-shaped plate crystals. The crystals are air-sensitive when finely ground.

X-ray structural analysis of $RbCe_3Te_8$: crystal dimensions $0.225 \times 0.446 \times 0.022$ mm, monoclinic, $P2_1/a$ (No. 14), $Z = 4$, $a = 9.051(2)$ Å, $b = 12.996(3)$ Å, $c = 14.376(3)$ Å, $\beta = 98.87(2)°$, $V = 1670.8(7)\,Å^3$, $\rho_{calc} = 6.069\,g\,cm^{-3}$, $2\theta_{max} = 50°$, Mo$K\alpha$ radiation, $\lambda = 0.71069$ Å, ω–2θ scan mode, $T = 23°C$, 3301 reflections measured, 3096 unique reflections, data corrected for Lorentz–polarization effects and for absorption (based on ψ scans), $\mu(MoK\alpha) = 232.41\,cm^{-1}$, solution by direct methods, anisotropic refinement on F by full-matrix least squares, 110 parameters, $R = 0.058$, $R_w = 0.072$ for 1565 reflections having $F_o^2 > 3\sigma(F_o^2)$, min/max residual electron density $= -5.33\,e\,Å^{-3}/5.13\,e\,Å^{-3}$.

3. **KNd_3Te_8** was synthesized from a mixture of K_2Te (1.0 mmol), Cu (0.5 mmol), Nd (0.5 mmol), and Te (4.5 mmol) that was sealed under vacuum in a carbon-coated quartz tube, heated to 850°C for 6 days, cooled to 300°C at $4°C\,h^{-1}$, and quenched to room temperature. The excess K_xTe_y flux was removed with DMF to reveal silver hexagonal-shaped plate crystals. The crystals are air-sensitive when finely ground.

X-ray structural analysis of KNd_3Te_8: crystal dimensions $0.181 \times 0.207 \times 0.026$ mm, monoclinic, $P2_1/a$ (No. 14), $Z = 4$, $a = 8.956(1)$ Å, $b = 12.836(2)$ Å, $c = 13.856(3)$ Å, $\beta = 99.420(2)°$, $V = 1571.4(8)\,Å^3$, $\rho_{calc} = 6.308\,g\,cm^{-3}$, $2\theta_{max} = 50°$, Mo$K\alpha$ radiation, $\lambda = 0.71069$ Å, ω–2θ scan mode, $T = -85°C$, 2373 reflections measured, 2200 unique reflections, data corrected for Lorentz–polarization effects and for absorption (based on ψ scans), $\mu(MoK\alpha) = 246.40\,cm^{-1}$, solution by direct methods, anisotropic refinement on F by full-matrix least squares, 110 parameters, $R = 0.054$, $R_w = 0.062$ for 768 reflections having $F_o^2 > 3\sigma(F_o^2)$, min/max residual electron density $= -2.90\,e\,Å^{-3}/2.30\,e\,Å^{-3}$. The final fractional atomic coordinates and average isotropic temperature factors are given in Table 1.

TABLE 1
Positional Parameters and B (eq) for KNd_3Te_8

Atom	x	y	z	B_{eq} (Å^2)[a]
Nd1	0.6042(3)	0.4106(3)	0.8492(2)	0.8(1)
Nd2	0.9299(3)	0.5795(3)	0.1476(2)	0.8(1)
Nd3	0.9141(2)	0.254(1)	0.1548(2)	1.5(1)
Te1	0.8607(4)	0.5804(3)	0.9176(3)	1.4(1)
Te2	0.6544(4)	0.4143(4)	0.0933(3)	1.2(1)
Te3	0.8533(3)	0.245(1)	0.9167(2)	1.5(1)
Te4	0.9473(4)	0.4179(3)	0.3268(3)	1.6(1)
Te5	0.7102(4)	0.2777(2)	0.3411(3)	1.4(1)
Te6	0.4690(4)	0.4227(3)	0.3409(3)	1.5(1)
Te7	0.2076(4)	0.5967(3)	0.3303(3)	1.7(1)
Te8	0.0423(3)	0.247(1)	0.6704(2)	1.7(1)
K1	0.259(1)	0.409(1)	0.5357(9)	2.4(4)

[a] Anisotropically refined atoms are given in the form of the isotropic equivalent displacement parameter defined as $B_{eq} = (8\pi^2/3)[a^2B_{11} + b^2B_{22} + c^2B_{33} + ab(\cos\gamma)B_{12} + ac(\cos\beta)\ B_{13} + bc(\cos\alpha)B_{23}]$. The anisotropic temperature factor expression is $\exp[-2\pi^2(B_{11}a^{*2}h^2 + \cdots + 2B_{12}\,a^*b^*hk + \cdots)]$.

ACKNOWLEDGMENTS

Financial support from the National Science Foundation (Grants DMR-9527347 (M.G.K.) and DMR-9622025 (C.R.K.)) is gratefully acknowledged. M.G.K. is a Henry Dreyfus Teacher–Scholar (1993–1998). This work made use of the SEM and TEM facilities of the Center for Electron Optics at Michigan State University.

REFERENCES

1. M. Erlander, G. Hägg, and A. Westgren, *Ark. Kemi, Mineral. Geol.* **12B**(1), 1 (1935).
2. A. J. K. Haneveld and F. Jellinek, *Recl. Trav. Chim. Pays-Bas* **83,** 776 (1964).
3. P. Boher, P. Garnier, J. R. Gavarri, A. W. Hewat, *J. Solid State Chem.* **57,** 343 (1985).
4. (a) K. R. Andress and E. Alberti, *Z. Metallkd* **27**(6), 126 (1935); (b) D. K. Das and D. T. Pitman, *Trans. Am. Inst. Min., Metall. Pet. Eng.* **209,** 1175 (1957).
5. Z. Ban and M. Sikirica, *Acta Crystallogr.* **18,** 594 (1965).
6. C. Zheng and R. Hoffmann, *J. Am. Chem. Soc.* **108,** 3078 (1986).
7. (a) E. Brechtel, G. Cordier, and H. Z. Schäfer, *Z. Naturforsch., B: Anorg. Chem., Org. Chem.* **34,** 251 (1979); *Z. Naturforsch., B: Anorg. Chem., Org. Chem.* **35,** 1 (1980); *J. Less-Common Met.* **79,** 131 (1981); (b) G. Cordier, B. Eisenmann, and H. Z. Schäfer, *Z. Anorg. Allg. Chem.* **426,** 205 (1976); (c) G. Cordier and H. Z. Schäfer, *Z. Naturforsch., B: Anorg. Chem., Org. Chem.* **32,** 383 (1976); (d) N. May and H. Z. Schäfer, *Z. Naturforsch., B: Anorg. Chem., Org. Chem.* **29,** 20 (1974); (e) W. Dorrscheidt, G. Savelsberg, J. Stöhr, and H. Z. Schäfer, *J. Less Common Met.* **83,** 269 (1982).
8. (a) $LnNi_2Si_3$ (Ln = Sc, U): B. Ya. Kotur, O. I. Bodak, and E. I. Gladyshevski, *Sov. Phys. Crystallogr.* **23,** 101 (1978); (b) $ScNiSi_3$: B. Ya. Kotur, O. I. Bodak, M. G. Mys'kiv, and E. I. Gladyshevskii, *Sov. Phys. Crystallogr.* **22,** 151 (1977); (c) $SmNiGe_3$: O. I. Bodak, V. K. Pecharskii, O. Ya. Mruz, V. Yu. Zarodnik, G. M. Vivits'ka, and P. S. Salamakha, *Dopov. Akad. Nauk Ukr. RSR, Ser. B.* **2,** 36 (1985).
9. (a) W. Lin, H. Steinfink, and F. Weiss, *Inorg. Chem.* **4,** 877 (1965); R. Wang, H. Steinfink, and W. F. Bradley, *Inorg. Chem.* **5,** 142 (1966); (b) M.-P. Pardo, J. Flahaut, and L. C. R. Domange, *Bull. Soc. Chim. Fr.* 3267 (1964); (c) T. H. Ramsey, H. Steinfink, and E. Weiss, *Inorg. Chem.* **4,** 1154 (1965); (d) B. K. Norling and H. Steinfink, *Inorg. Chem.* **5,** 1488 (1966).
10. J. Cody and J. Ibers, *Inorg. Chem.* **35,** 3836 (1966).
11. X. Zhang, J. Li, S. Foran, H.-Y. Guo, T. Hogan, C. R. Kannewurf, and M. G. Kanatzidis, *J. Am. Chem. Soc.* **117,** 10513 (1995).
12. W. J. Sheldrick and M. Wachhold, *Angew. Chem.* **107,** 490 (1995); *Angew. Chem., Int. Ed. Engl.* **34,** 40 (1995).
13. M. G. Kanatzidis, *Angew. Chem.* **107,** 2281 (1995); *Angew. Chem., Int. Ed. Engl.* **34,** 2109 (1995).
14. G. Savelsberg and H. Schäfer, *Z. Naturforsch, B* **33,** 370 (1978).
15. S. Lee and B. Foran, *J. Am. Chem. Soc.* **116,** 154 (1994).
16. B. Foran, S. Lee, and M. Aronson, *Chem. Mater.* **5,** 974 (1993).
17. J. C. Huffman and R. C. Haushalter, *Z. Anorg. Allg. Chem.* **518,** 203 (1984).
18. N. N. Greenwood and A. Earnshaw, *Chemistry of the Elements*, Pergamon Press, New York, 1984, p. 1443.